Article

Cell Chemical Biology

Locally Activating TrkB Receptor Generates Actin Waves and Specifies Axonal Fate

Graphical Abstract

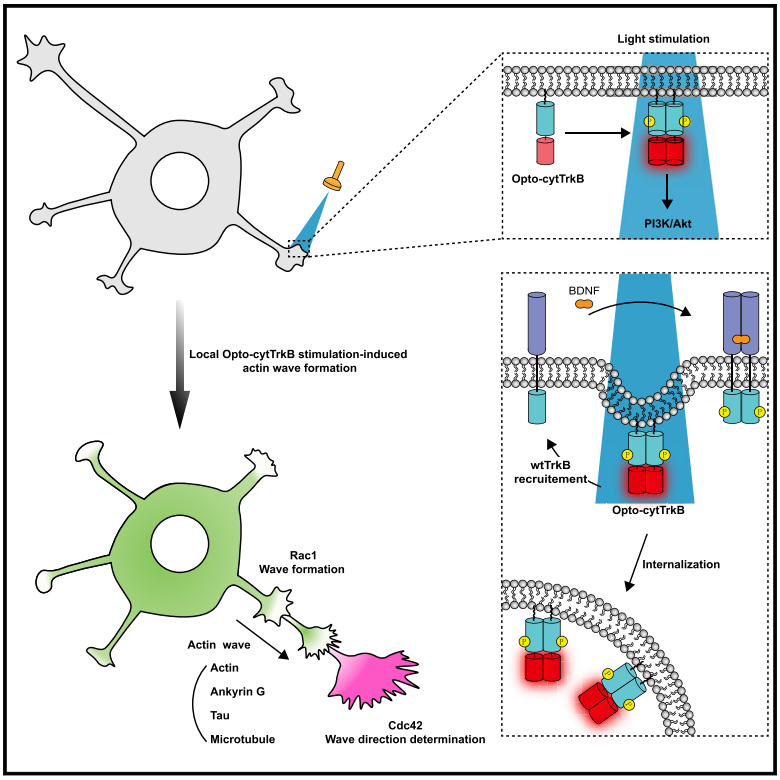

Highlights

- The photoactivatable TrkB receptors initiate actin waves in developing neurons
- Activated TrkB generates actin waves through the PI3K/AKT pathway
- Activated TrkB at the neurite end mediates Rac1 signaling from the cell body
- Local TrkB activation recruits key axonal proteins to the stimulated neurite

Authors

Doyeon Woo, Yeji Seo, Hyunjin Jung, ..., Sangkyu Lee, Kwang-Hyun Cho, Won Do Heo

Correspondence

ckh@kaist.ac.kr (K.-H.C.), wondo@kaist.ac.kr (W.D.H.)

In Brief

Actin waves are the drivers to transport axon-promoting factors, yet its upstream regulator remains elusive. Using Opto-cytTrkB system, Woo et al. delineate the role of TrkB signaling on actin waves. They report that axonal molecules relocate to the TrkB-activated neurite, allowing that neurite to acquire an axonal property.

Woo et al., 2019, Cell Chemical Biology *26*, 1–12
December 19, 2019
https://doi.org/10.1016/j.chembiol.2019.10.006

CellPress

Please cite this article in press as: Woo et al., Locally Activating TrkB Receptor Generates Actin Waves and Specifies Axonal Fate, Cell Chemical Biology (2019), https://doi.org/10.1016/j.chembiol.2019.10.006

Cell Chemical Biology
Article

Locally Activating TrkB Receptor Generates Actin Waves and Specifies Axonal Fate

Doyeon Woo,[1,4] Yeji Seo,[2,4] Hyunjin Jung,[2] Sungsoo Kim,[2] Nury Kim,[1] Sang-Min Park,[3] Heeyoung Lee,[1] Sangkyu Lee,[1] Kwang-Hyun Cho,[3,*] and Won Do Heo[1,2,5,*]
[1]Center for Cognition and Sociality, Institute for Basic Science (IBS), Daejeon 34141, Republic of Korea
[2]Department of Biological Sciences, Korea Advanced Institute of Science and Technology (KAIST), Daejeon 34141, Republic of Korea
[3]Department of Bio and Brain Engineering, Korea Advanced Institute of Science and Technology (KAIST), Daejeon 34141, Republic of Korea
[4]These authors contributed equally
[5]Lead Contact
*Correspondence: ckh@kaist.ac.kr (K.-H.C.), wondo@kaist.ac.kr (W.D.H.)
https://doi.org/10.1016/j.chembiol.2019.10.006

SUMMARY

Actin waves are filamentous actin (F-actin)-rich structures that initiate in the somato-neuritic area and move toward neurite ends. The upstream cues that initiate actin waves are poorly understood. Here, using an optogenetic approach (Opto-cytTrkB), we found that local activation of the TrkB receptor around the neurite end initiates actin waves and triggers neurite elongation. During actin wave generation, locally activated TrkB signaling in the distal neurite was functionally connected with preferentially localized Rac1 and its signaling pathways in the proximal region. Moreover, TrkB activity changed the location of ankyrinG—the master organizer of the axonal initial segment-and initiated the stimulated neurite to acquire axonal characteristics. Taken together, these findings suggest that local Opto-cytTrkB activation switches the fate from minor to major axonal neurite during neuronal polarization by generating actin waves.

INTRODUCTION

During neuronal growth and development, neurons undergo a morphological transition from a multi-polar intermediate state, characterized by short, extended immature neurites, to a state in which each neurite has the potential to develop into a dendrite or an axon (Barnes and Polleux, 2009; Dotti et al., 1988). Immature neurites have growth cones at their tips that can elongate. Actin filaments in these tips undergo rapid polymerization and depolymerization (Baas and Buster, 2004; Dent and Gertler, 2003). Developing neurons initially form equivalent immature neurites, but eventually one neurite grows faster than the others and becomes the axon, whereas the remaining neurites polarize and develop into dendrites (Arimura and Kaibuchi, 2007). Neuronal polarization occurs via several intracellular signaling pathways that act by regulating cytoskeletal structures (Schelski and Bradke, 2017). Brain-derived neurotrophic factor (BDNF)-TrkB signaling is one of the main axes involved in this process. Extracellular BDNF acts through binding to its receptor, TrkB, to induce an increase in cAMP that promotes axon differentiation in cultured neurons via a self-amplifying autocrine mechanism (Cheng et al., 2011). In cytoskeletal structures undergoing polarization, actin is less rigid and growth cones are larger in future axonal neurites than in other, minor neurites before initiation of axon growth (Bradke and Dotti, 1999; Stiess and Bradke, 2011). Interestingly, it has been reported that undifferentiated neurites can exhibit growth cone-like waves, also called actin waves (Flynn et al., 2009; Ruthel and Banker, 1998, 1999; Winans et al., 2016). Some researchers have suggested that actin waves increase axonal transport and are more prevalent in future potent axons (Ruthel and Banker, 1998). However, the process that initiates growth cone-like waves remains unknown. The mechanism by which extracellular cues and/or membrane receptors determine axonal and dendritic fate is also unclear. Indeed, researchers have strived for decades to pinpoint the factors that drive neuronal polarity and explain how a single neurite is selected to become an axon.

To obtain polarity, neurons must possess two distinct morphological and functional characteristics. They also require diffusion barriers called axon initial segments (AIS), which have two essential roles: maintaining axonal identity and generating action potentials (Rasband, 2010). AnkyrinG (AnkG), one of the known AIS molecules, is critical for AIS assembly and maintaining neuronal polarity (Gasser et al., 2012; Hedstrom et al., 2008; Jenkins and Bennett, 2001; Ogawa and Rasband, 2008). However, it is unclear whether actin waves affect the axon determination process, such as axonal protein transport and AIS assembly due to the lacking of the technique to induce actin waves in space and time.

Here, we demonstrated that locally activating BDNF-TrkB signaling is essential for proper neuronal polarity and further investigated its effects on neuronal polarity. For these investigations, we used an optogenetic technique employing the light-activated module, Opto-cytTrkB, which regulates the TrkB receptor activity. The Opto-cytTrkB system enables us to examine and comprehend elaborate cellular mechanisms in fine spatiotemporal detail (Chang et al., 2014; Kim et al., 2019). We found that local TrkB activation at neurite tips causes gathering of filamentous actin (F-actin) and initiation of growth cone-like actin waves, ultimately leading to neurite elongation. Actin waves and neurite elongation are regulated by the activities

of the Rho GTPases, Cdc42 and Rac1. Intriguingly, we revealed that endogenous Cdc42 and Rac1 shows differential localization within the cell, and consequently contributes to different aspects of actin wave occurrence in TrkB-activated neurite. Using a photo-activated Rac1 system, we also found that activated TrkB signaling at neurite tips is functionally linked with Rac1-mediated signaling pathways at the proximal neurite, and thereby generates actin waves. Local TrkB-triggered actin dynamics act through this molecular mechanism can also induce growth cone formation at neurite tips and promote neurite elongation. Furthermore, local TrkB-activation caused relocation of AnkG, the master organizer of the AIS. Taken together, these findings suggest that local activation of Opto-cytTrkB through blue light illumination generates actin waves, which convert minor axonal neurites to major axonal neurites during neuronal polarization.

RESULTS

Local TrkB-Induced Actin Waves and Neurite Elongation

Autocrine BDNF signaling in neurons acts by triggering cAMP and protein kinase A activity to play a role in axon development (Cheng et al., 2011). Here, we found that BDNF-TrkB signaling during early neuronal development is essential for proper neuronal elongation (Figures S1A and S1B). BDNF-treated neurons also exhibited larger growth cones and growth cone-like wave structures in the middle of neurites; notably, growth cones were lost upon sequestration of BDNF with a BDNF antibody (Figures S1C and S1D). It has been reported that BDNF also enhances the formation of actin waves during axonal regeneration (Difato et al., 2011). We thus explored the effect of BDNF stimulation on actin wave formation in developing neurons by expressing LifeAct, which allows visualization of F-actin structures (Riedl et al., 2008). BDNF stimulation induced formation of dynamic, global actin waves, which enhanced neurite elongation and caused high accumulation of F-actin (Figures S1E and S1F; Video S1). To address the local effect of BDNF on neuronal development, we applied the Opto-cytTrkB system, a previously developed optogenetic approach (Chang et al., 2014; Kim et al., 2019) that allows TrkB to be activated in the absence of interactions with its endogenous ligand, BDNF (Figure 1A). At 2 days *in vitro* (DIV2), a time when cultured neurons expressed both mCherry-LifeAct and Opto-cytTrkB, we stimulated neurons locally with light two times for 20 min each. Local light stimulation induced F-actin accumulation around light-stimulated areas (Figure 1B; Video S2). A quantitative analysis of F-actin intensity indicated that local Opto-cytTrkB activation triggered significant actin accumulation in the light-stimulated neurite. By contrast, F-actin intensity was diminished in the unstimulated neurite (Figure 1C).

Administration of a light stimulus, specifically at the restricted areas of growth cone structures, caused an F-actin-rich wave to emerge from the somatodendritic area and travel to the neurite end, leading to neurite elongation (Figure 1D). Repeated administration of light to activate local Opto-cytTrkB around the growth cone area caused repeated creation of actin waves, which in turn accelerated neurite elongation (Figure 1E; Video S3). During this process, unstimulated neurites exhibited a decrease in both length and F-actin signals. A quantitative analysis suggested that the length of stimulated neurites increased by ~1.5-fold compared with that of unstimulated neurites (Figure 1F). These results demonstrate that Opto-cytTrkB-induced actin wave formation leads to neurite elongation and causes F-actin to accumulate at high concentrations at the end of the stimulated neurite. We then analyzed changes in neurite length during repeated local TrkB stimulation. Interestingly, neurite length decreased immediately after light stimulation, but rebounded by the end of the 30-min light-on phase. Then neurite elongation was accelerated efficiently after the light-on phase (Figure 1G). It is known that BDNF induces neurite retraction in cultured spinal neurons from *Xenopus* within 1 min after BDNF addition through a Ca^{2+}-signaling-dependent mechanism (Wang and Zheng, 1998). Thus, the reduction in neurite length observed immediately after light was applied would depend on Ca^{2+} signaling mediated by the local Opto-cytTrkB activation. Next, we further validated the specificity of local light stimulation. We found that delivery of a local light stimulus to the midpoint between two adjacent growth cones caused no detectable changes in actin signal, confirming that light did not leak out from the target area and affect other neuronal regions. Only activating TrkB locally at the neurite end (i.e., growth cone) induced actin wave formation, which in turn caused neurite elongation, demonstrating the region specificity of our light stimulation condition (Figure S1G; Video S4). Notably, we also confirmed that actin waves could not be generated using Opto-cytTrkB containing a light-insensitive CRY2PHR mutant (D387A), indicating that the observed effects were not attributable to photo-toxicity or other off-target, TrkB-independent effects of sustained light stimulation (Figures S1H and S1I). Taken together, these findings suggest that local TrkB activity triggered by engaging the Opto-cytTrkB system regulates the formation of actin waves that emerge from the proximal area close to the soma.

Formation of Growth Cones through an Imbalance in Actin

During neuronal development, stage 2 neurons possess several neurites with growth cones at their ends. One neurite typically grows much faster than the other neurites, supporting neurite extension and ultimately leading to neuronal polarity (Arimura and Kaibuchi, 2007). Using Opto-cytTrkB receptors, we created a growth cone in one particular neurite (Figure 2A). To accomplish this, we expressed Opto-cytTrkB together with mCherry-LifeAct in DIV2 neurons and chose a stage 2 neuron to activate local TrkB receptors in a neurite lacking a growth cone. Among the multiple neurites with several growth cone structures at the ends, light illumination strongly activated local TrkB specifically at the end of a neurite that did not possess growth cones. This led to the formation of a growth cone. Accumulated F-actin around this growth cone was persistently maintained at the neurite's end, accelerating elongation of the neurite. By contrast, most growth cones that existed before stimulation vanished altogether. Quantification of changes in the appearance and disappearance of growth cones revealed an 80% increase in growth cones in TrkB-activated neurites compared with unstimulated neurites (Figure 2B). In addition, stimulated neurites exhibited more than a 3.5-fold increase in total growth cone area compared with the original states of growth cones before light stimulation (Figure 2C).

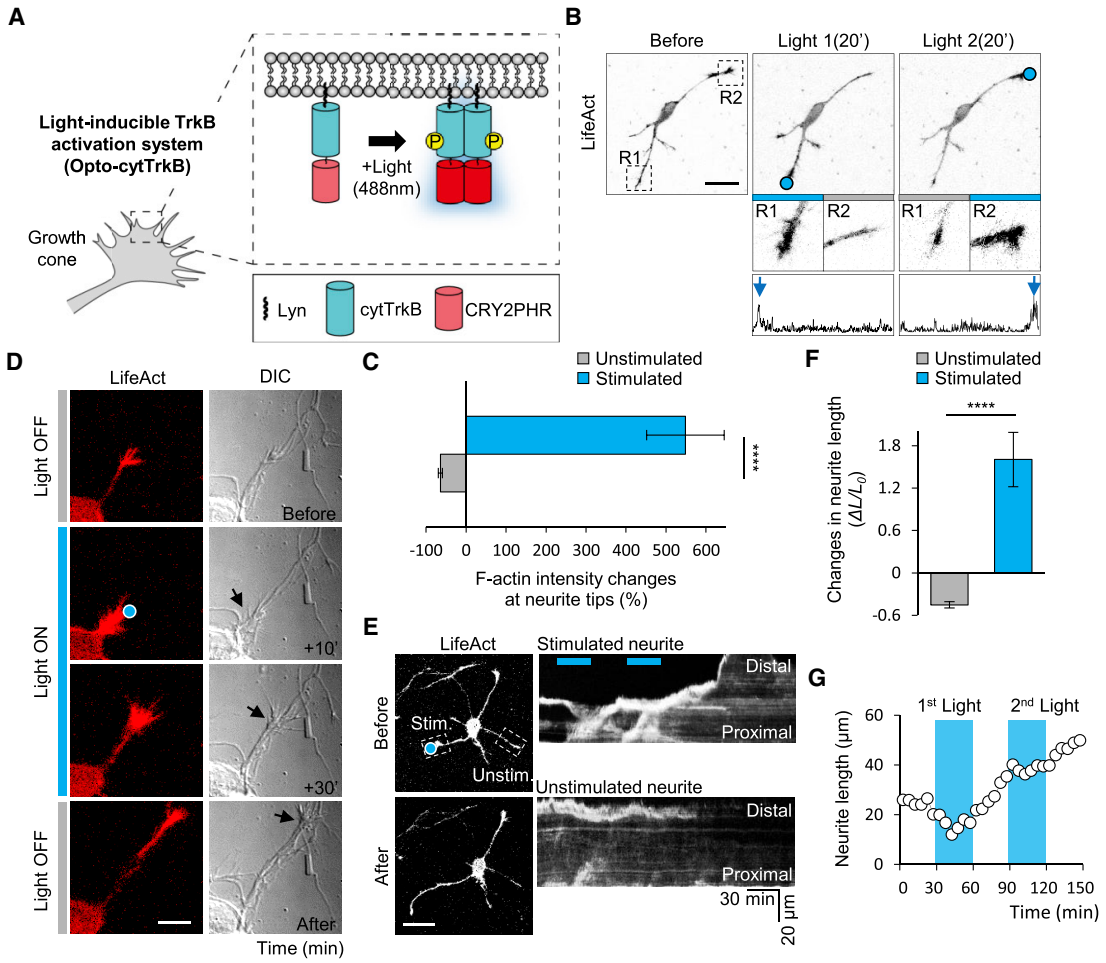

Figure 1. F-Actin Wave Generation and Neurite Elongation by Light-Mediated Local TrkB Activation

(A) Schematic illustration depicting the Opto-cytTrkB activating system using Lyn (myristoylation signal peptide), cytTrkB (cytoplasmic domain of TrkB), and CRY2PHR (PHR domain of cryptochrome2).

(B) Immature hippocampal neurons expressing LifeAct (F-actin) together with Opto-cytTrkB locally stimulated with blue light. Top: two different growth cone stimulation areas (R1 and R2) before light stimulation (left panel) and after a 20-min light stimulation (right panels). The blue circles indicate the light-stimulated area. Middle: magnification of boxed areas in the upper left panel showing F-actin in each growth cone. Blue and gray bars indicate light-stimulated and unstimulated growth cones, respectively. Bottom: intensity plots showing increased F-actin fluorescence intensity (blue arrows). Scale bar, 20 μm.

(C) Changes in F-actin intensity in Opto-cytTrkB-stimulated and unstimulated neurites in a single hippocampal neuron. Data show the percentage change in F-actin intensity at neurite tips, presented as means ± SEM (n > 35; ****p < 0.0001; two-tailed t test).

(D) Local F-actin-rich wave arising from the somatodendritic area in response to Opto-cytTrkB activation. The blue circle indicates the light-illuminated area in LifeAct images; black arrows mark actin wave movement in differential interference contrast (DIC) images. Scale bar, 10 μm.

(E) Left: LifeAct images of a neuron before and after light stimulation, showing neurite elongation induced by local Opto-cytTrkB activation (blue circle). Right: kymographs of F-actin in the stimulated neurite showing actin wave formation and movement in response to two different repetitive light stimulation periods (blue bars). Scale bar, 25 μm.

(F) Changes in neurite length in stimulated versus unstimulated neurites in the same hippocampal neurons after local Opto-cytTrkB activation ($\Delta L/L_0$; L, length). Data are presented as means ± SEM (n > 25; ****p < 0.0001; two-tailed t test).

(G) Neurite elongation kinetics before, during, and after light-stimulating periods (blue areas) in Opto-cytTrkB-expressing hippocampal neurons (DIV2–3).

See also Figure S1 and Videos S1, S2, S3, and S4.

Next, we explored whether the total amount of actin—including globular (G)- and F-actin—changed under different conditions, including F-actin accumulation, neurite elongation, and growth cone formation, in developing (unpolarized) neurons. An examination of DIV2 neurons expressing both Opto-cytTrkB and actin-mCherry for detection of G- and F-actin, showed that activation of local TrkB by light stimulation caused actin enrichment and led to neurite elongation (Figure 3A). We then analyzed total actin intensity profiles in line scans of the whole cell area (Figure 3B). We found that before light illumination, most actin was present on the left side of the soma. During the light-on phase, actin intensity shifted toward the local TrkB-activated area and diminished in the pre-enriched growth cone area. After turning off the light, the accumulated actin traveled externally in the form of waves and induced neurite elongation. However, the amount of total actin before and after light

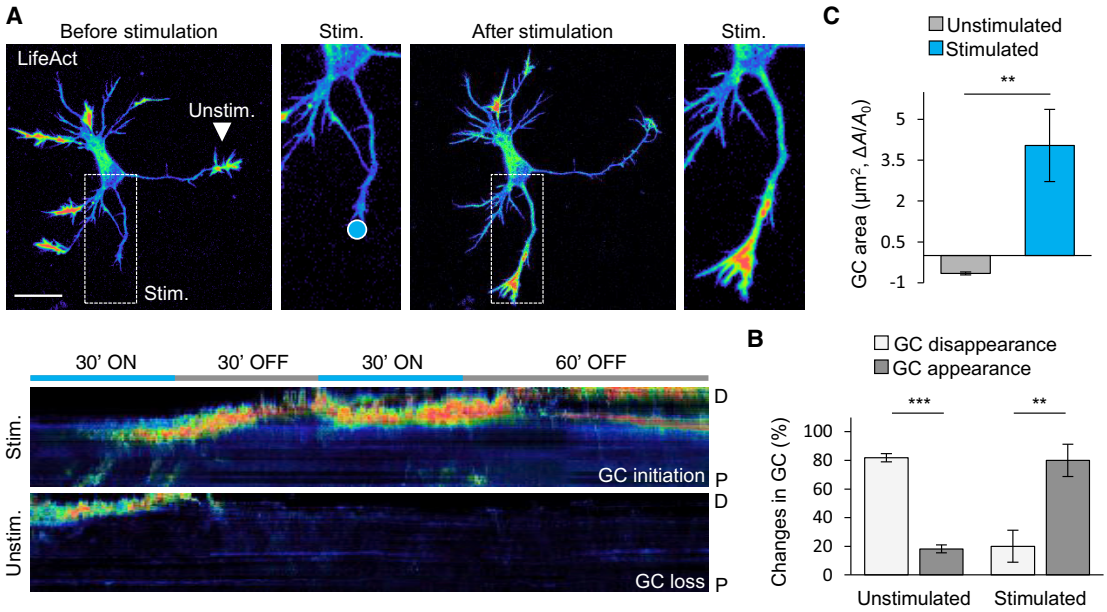

Figure 2. Local Opto-cytTrkB-Induced Growth Cone Formation

(A) Cultured young hippocampal neurons (DIV2–3) with multiple growth cones at the tips of neurites, co-expressing Opto-cytTrkB and iRFP682-LifeAct. Opto-cytTrkB was activated locally by light stimulation of the area indicated by a blue circle. Kymographs show growth cone (GC) initiation and loss during the indicated 30-min on and 30- and 60-min off periods. Blue bars, light-on period; gray bars, light-off period. Scale bar, 25 μm.

(B) Quantification of growth cone appearance and disappearance. Data show percent changes, presented as means ± SEM (n = 20; ***p = 0.0007, **p = 0.0054; two-tailed t test).

(C) Changes in growth cone area in stimulated and unstimulated neurites in the same hippocampal neurons after local Opto-cytTrkB activation ($\Delta A/A_0$; A, area; μm^2). Data are presented as means ± SEM (n > 20; **p = 0.0021; two-tailed t test).

stimulation remained unaltered (Figure 3C). We also found little involvement of protein synthesis in actin remodeling induced by local TrkB activation (Figures 3D and 3E). There was no significant difference in total actin or F-actin accumulation, as detected using the Opto-cytTrkB system, in DIV2–3 neurons pre-incubated with the protein synthesis inhibitors anisomycin (100 μM) or cycloheximide (100 mg/mL). Thus, local activation of TrkB in neurites regulates actin dynamics without affecting the actin pool. Taken together, these findings suggest that locally elevated TrkB activity affects growth cone formation and enables neurite elongation.

Local Self-Amplifying BDNF-TrkB Signaling in Opto-cytTrkB-Mediated Actin Modulation

To investigate how light stimulation of Opto-cytTrkB induces actin waves and growth cone formation, we speculated that local BDNF-TrkB-positive feedback mechanisms are involved in light-induced actin modulation (Figure S2A). To determine this, we simplified the TrkB-signaling network while preserving the positive feedback loop. Our TrkB network model consisted of four nodes: (1) TrkB, which is activated by BDNF; (2) Opto-cytTrkB, which is independently activated by light stimulation; (3) the phosphatidylinositol 3-kinase (PI3K)/Akt pathway, which is activated by both TrkB and Opto-cytTrkB; and (4) BDNF release, which is increased by PI3K/Akt signaling. We tested whether these nodes contribute to eliciting the specific output response of F-actin enrichment at the light-illuminated neurite. To this end, we delivered local light stimulation to a neuron co-expressing Opto-cytTrkB and BDNF-FusionRed or BDNF-pHTomato. The pH-sensitive fluorescence protein was used to monitor the BDNF secretion through intensity changes. Using BDNF conjugated with two kinds of fluorescence proteins, we observed that BDNF specifically accumulated in the local TrkB-activated area and it was released at the neurite end that received light (Figures S2B and S2C). The same experiment was then performed in neurons co-expressing Opto-cytTrkB and wild-type TrkB-FusionRed. Upon local light illumination, wild-type TrkB receptors appeared to be recruited to the illuminated area (Figures S2D and S2E). Furthermore, blocking BDNF induced a decrease in the accumulation of F-actin upon local TrkB activation (Figures S2F and S2G). In developing neurons, TrkB receptors, which are activated by BDNF binding, are internalized and transported to the cell body through retrograde vesicle trafficking (Segal, 2003). Thus, we also monitored Rab7-mediated retrograde vesicle transport upon light stimulation. Retrograde movement of Rab7 was detected specifically in the TrkB-activated neurite, and not in the unstimulated neurite (Figure S3A). Moreover, neurotrophin-interacting receptors were internalized and moved in a retrograde direction with Rab7 both BDNF- and light-treated conditions (Figures S3B and S3C). Collectively, our findings suggest that Opto-cytTrkB modulates F-actin in growth cone areas through a local BDNF-TrkB-positive feedback mechanism (Figure S3D).

Preferential Localization of Cdc42 and Rac1 for Actin Waves

To further investigate the signaling pathway involved in local TrkB-triggered actin waves, we tested several different

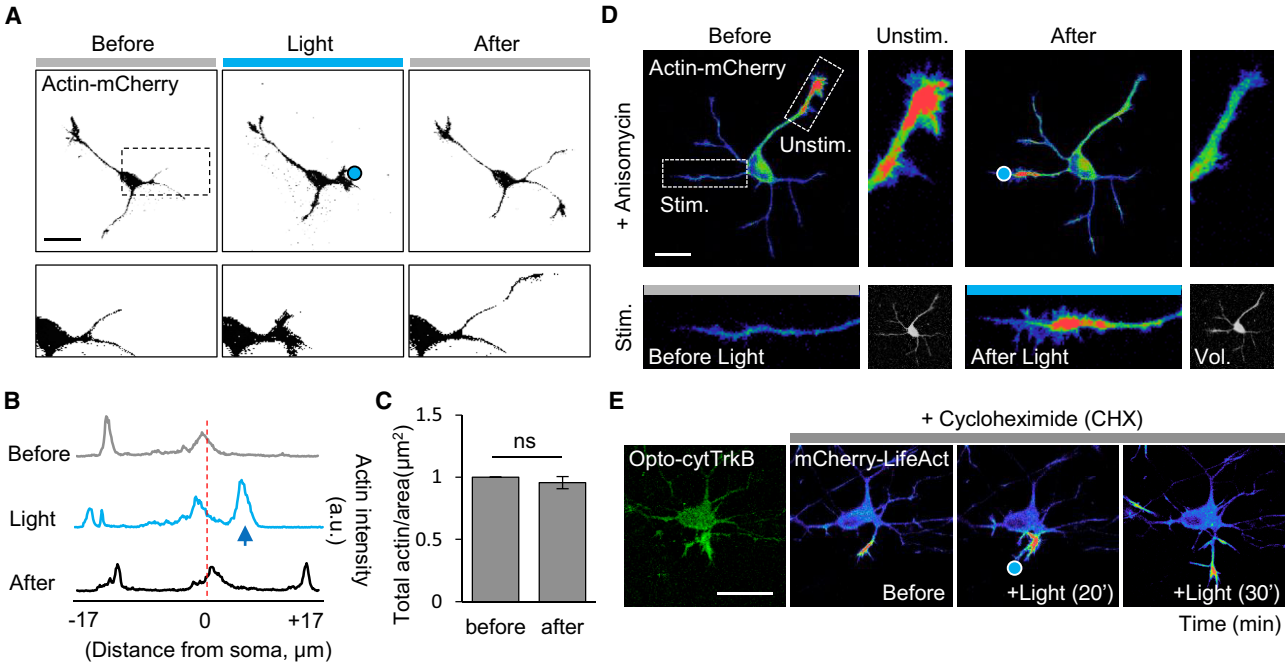

Figure 3. Neurite Elongation and Growth Cone Formation by Actin Imbalance

(A) Young neurons expressing Opto-cytTrkB and actin-mCherry before, during, and after light stimulation. The blue circle indicates the light-stimulated area. Scale bar, 25 μm.

(B) Actin intensity profiles from (A), 30 min before and 30 min after the light stimulation period. The blue arrow indicates the light-stimulated area.

(C) Summary data showing total actin intensity before and after local Opto-cytTrkB activation, expressed as the ratio of actin-mCherry intensity to neuronal area (μm^2). Data are presented as means ± SEM (n = 12; ns, not significant; two-tailed t test).

(D) Cultured neurons at DIV2–3 expressing Opto-cytTrkB-2A-iRFP682 and actin-mCherry were treated with anisomycin to block protein translation. Anisomycin (100 μM) was pre-incubated for 1 h before local TrkB activation. The blue circle indicates the light-stimulated area. The iRFP682 signal was used as a volume control (gray images). Bottom: magnified images before (gray bar) and after (blue bar) local TrkB activation using the Opto-cytTrkB system. Scale bar, 25 μm.

(E) Cycloheximide (100 mg/mL) was used to inhibit protein synthesis in Opto-cytTrkB and mCherry-LifeAct-expressing neurons. Cycloheximide was pre-incubated for 1 h before local TrkB activation. The blue circle indicates the light-stimulated area. Scale bar, 25 μm.

Opto-cytTrkB mutants that affect TrkB downstream signaling. There are three canonical signaling pathways downstream of TrkB: (1) PI3K/Akt; (2) mitogen-activated protein kinase (MAPK)/extracellular signal-regulated kinase (ERK); and (3) phospholipase Cγ1 (PLCγ1)/Ca^{2+}. These pathways function throughout the brain and contribute to neuronal survival, neurite outgrowth, and synaptic plasticity (Squinto et al., 1991). We used Opto-cytTrkB (Y515F) to inhibit both PI3K/Akt and MAPK/ERK pathways, and Opto-cytTrkB (Y816F) to block the PLCγ1/Ca^{2+} pathway; we also tested the kinase-dead mutant, Opto-cytTrkB (K571N) (Minichiello et al., 1998, 2002). F-actin accumulation was significantly decreased upon local light activation of Opto-cytTrkB (Y515F) compared with that observed in Opto-cytTrkB-activated cells (Figures S4A–S4C). In contrast, inhibiting the PLCγ1/Ca^{2+} pathway using Opto-cytTrkB (Y816F) had little effect on F-actin dynamics, such that these cells showed a high level of actin recruitment to the light-stimulated area (Figures S4D and S4E). It was significantly different with the response from the kinase-dead Opto-cytTrkB (K571N), which completely failed to induce any changes in F-actin. These results suggest that the observed actin modulation was mediated by TrkB activation through phosphorylation of the Y515 residue, which is responsible for activating both PI3K/Akt and MAPK/ERK pathways. To verify which of these pathways was critical for TrkB-mediated actin modulation, we tested the effects of light illumination in the presence of the inhibitors, LY294002 (PI3K inhibitor) or PD0325901 (MAPK inhibitor). Inhibition of PI3K activity strongly suppressed actin wave generation in neurites (Figures 4A and 4B). In contrast, blocking the MAPK/ERK pathway had no effect on F-actin accumulation or actin wave generation (Figure 4C). These results thus demonstrate that the PI3K/AKT signaling pathway, rather than the MAPK/ERK pathway, is mainly involved in actin modulation downstream of TrkB activation (Figure 4D).

It has recently been reported that Rac-regulated actin polymerization generates spontaneous actin waves as a neuron undergoes various stages of growth and development (Winans et al., 2016). However, the endogenous localization of small GTPases and its effect on the appearance of local TrkB-dependent actin waves are not fully understood. We thus examined the effects of small GTPases on local TrkB-dependent actin modulation, which existed under the PI3K/AKT signaling pathway. We utilized an inducible protein translocation assay, based on hetero-interactions of FKBP (FK506 binding protein)-rapamycin-FRB (FKBP rapamycin binding) (Yang et al., 2012). To this end, we co-expressed Lyn-FRB, a plasma membrane-anchored form of FRB, and CFP-FKBP-GEF, a CFP (cyan fluorescent protein)-conjugated fusion protein of FKBP with a guanine

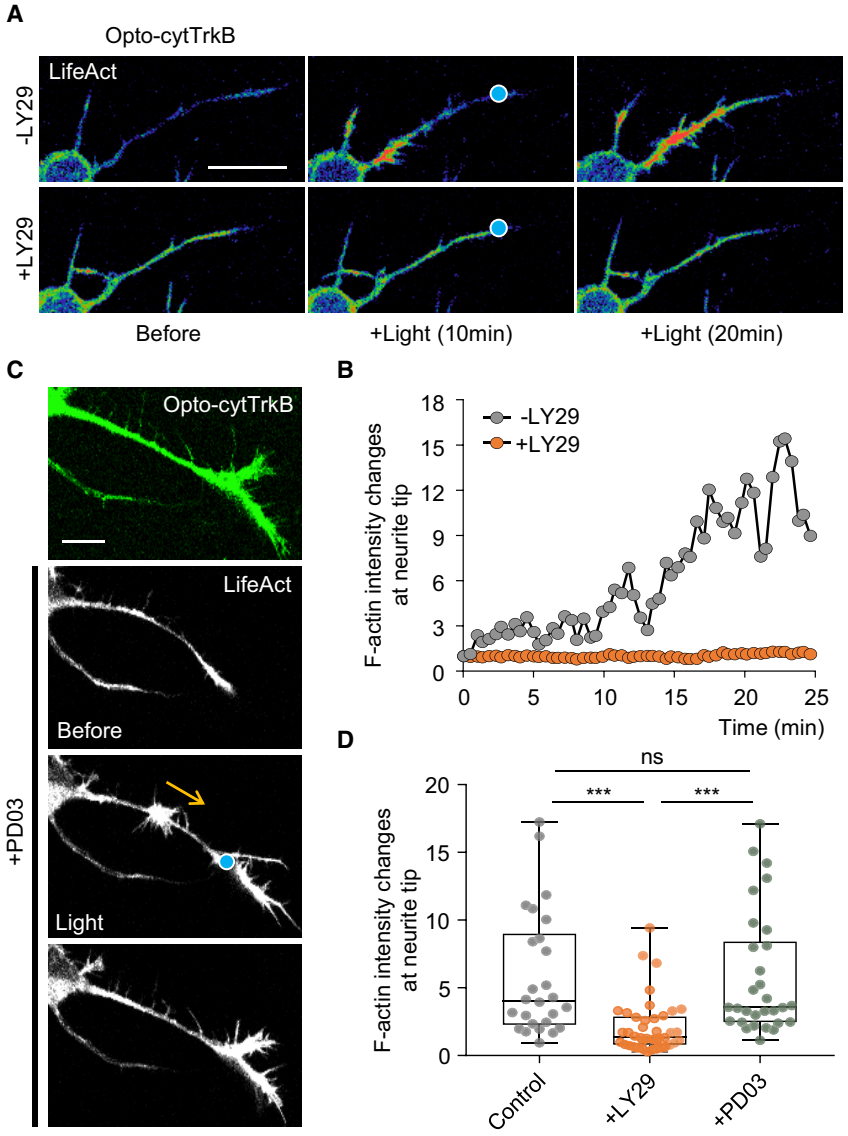

Figure 4. Involvement of PI3K/AKT Pathway on F-Actin Remodeling

(A) Prevention of actin wave formation by inhibition of PI3K/AKT using LY29 (100 μM, 30 min pre-incubation) in a local TrkB-activated neurite. The blue circle indicates the light-stimulated area. Scale bar, 20 μm.

(B) Changes in F-actin intensity in Opto-cytTrkB-stimulated neurites in single hippocampal neurons before and after inhibition of PI3K/AKT using LY29 (100 μM, 30 min pre-incubation).

(C) The actin wave generation in the ERK/MAPK inhibited neuron by using PD03 (50 nM, 30 min pre-incubation). The blue circle indicates the light-illuminated region; the arrow indicates the direction of actin wave movement. Scale bar, 10 μm.

(D) Quantification of changes in F-actin intensity ratio of Opto-cytTrkB stimulated neurite after pre-incubation of LY29 or PD03. Data are presented as means ± SEM (control, n = 26; LY29, n = 41; PD03, n = 30; ***p < 0.0003, ns, not significant; one-way ANOVA with Tukey multiple comparisons test).

See also Figures S2–S4.

nucleotide exchange factor (GEF) specific for Cdc42 (Fgd1), Rac1 (Tiam1), or RhoA (ARHGEF11) in cultured hippocampal neurons to activate each specific small GTPase at the plasma membrane (Figure S5A). In response to the rapamycin treatment, activated Cdc42 induced the formation of actin waves, whereas negative control cells expressing FKBP without a conjugated GEF did not induce any changes in F-actin signal (Figure S5B). By contrast, Rac1 activation caused formation of growth cone-like structures that dangled around neurites and generated actin waves that emerged near the soma and traveled toward the neurite ends. To obtain spatial information regarding Rac1 activity in actin wave generation, we applied a photoactivatable Rac1 (PA-Rac1) system (Wu et al., 2009). Interestingly, wave generation was highly efficient following activation of local Rac1 at the proximal neurite, but not following activation at intermediate or distal regions (Figures 5A–5C). This implies that locally activated TrkB signaling at neurite tips activates Rac1 signaling pathways in the proximal region, which mediates actin wave generation. To verify this, we monitored the localization of p21-activated kinase (Pak1) during Opto-cytTrkB activation. Pak1 is a well-characterized downstream effector of Rac1 that directly regulates actin polymerization (Edwards et al., 1999). Under local illumination of the neurite tip, Pak1 gradually moved from the cell body to the light-stimulated area in conjunction with the occurrence of actin waves (Figure S5C). Therefore, this result further supports our idea that activated TrkB receptors at the neurite tip are functionally linked with Rac1-mediated actin modulation at proximal neurites.

Next, to clearly delineate the role of Rac1 in local TrkB-mediated actin wave generation and movement, we locally activated TrkB in Rac1-inhibited neurons. Inhibition of Rac1 using NSC23766 decreased the occurrence of actin waves following local TrkB activation. However, actin waves still showed directional movement toward the ends of neurites (Figure S6A). This suggests the possibility that other signaling molecules are involved in actin wave formation, as well as movement, following local activation of TrkB by light stimulation of Opto-cytTrkB in growth cone areas. We hypothesized that local Cdc42 activity was necessary for induction of directional movement of emerging actin waves, as a traffic signal for movement. Inhibition of Cdc42 with the selective inhibitor, ZCL278, led to random movements of actin waves that emerged from a proximal neurite in unpolarized neurons in which TrkB was locally activated (Figure S6B). Taken together, these results suggest that Rac1 plays a predominant role in local TrkB-triggered actin wave formation, whereas Cdc42 is primarily responsible for TrkB activity-dependent directional movement of actin waves.

To investigate differences in subcellular localization between endogenous Cdc42 and Rac1, DIV2 hippocampal neurons

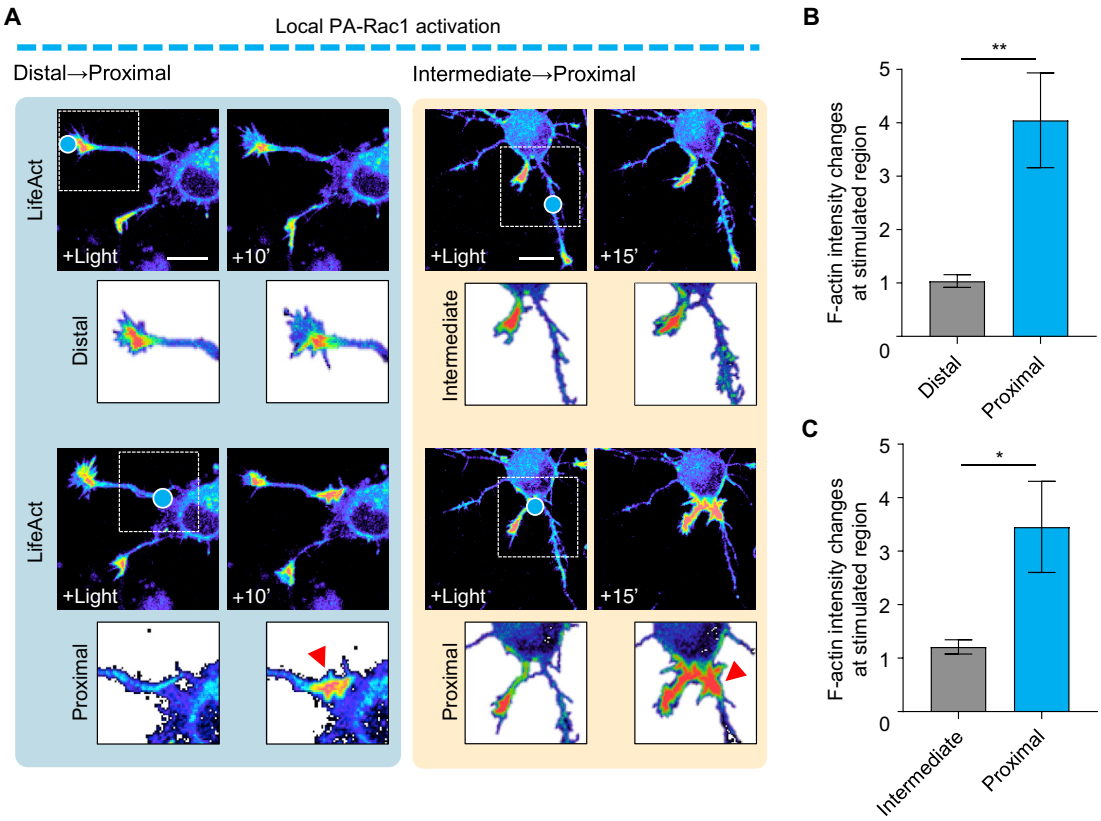

Figure 5. Efficient Actin Wave Formation at the Proximal Neurite

(A) Cultured hippocampal neurons co-expressing PA-Rac1 and mCherry-LifeAct. Left (blue box): neuron simulated at distal and proximal regions of the neurite. Right (yellow box): neuron stimulated at intermediate and proximal regions of the neurite. The blue circle marks the light-illuminated area. Magnified images of each stimulated area are displayed below the original images. Actin wave formation is indicated by a red arrowhead. Time (min). Scale bars, 15 μm.

(B) Changes in F-actin intensity at the distal and proximal region of the neurite, induced by activation of PA-Rac1. Data are presented as means ± SEM (n = 12; **p = 0.0028; two-tailed t test).

(C) Changes in F-actin intensity at intermediate and proximal regions of the neurite, induced by activation of PA-Rac1. Data are presented as means ± SEM (n = 21; *p = 0.0129; two-tailed t test).

See also Figures S5 and S6.

were immunostained for dendritic MAP2 protein and Cdc42 or Rac1, and also stained with phalloidin to visualize growth cones. We found that endogenous Cdc42 levels were higher in the soma, neurite shaft, growth cone, and neurite tips. By contrast, endogenous Rac1 was localized dominantly in the neurite shaft and soma (Figures 6A and 6B). To compare the differential localization of Cdc42 and Rac1, we quantified Cdc42 and Rac1 intensity in the neurite shaft and actin-enriched growth cones. Interestingly, Cdc42 staining was significantly more intense in neurite tips, whereas Rac1 showed weak localization to growth cones compared with neurite shafts (Figure 6C). Moreover, following local TrkB activation at the neurite tip, we observed propagation of fluorescence-tagged Rac1 toward the growth cone, together with actin waves (Figures S6C and S6D). Taken together, these data demonstrate that preferentially localized Cdc42 and Rac1 together with locally elevated TrkB activity regulates actin waves (Figure 6D).

Relocation of AnkG to the Local TrkB-Activated Neurite

The AIS is both a physical and physiological bridge between somato-dendritic and axonal domains, and is a crucial factor for maintaining the unique axonal environment (i.e., neuronal polarity). The master organizer of the AIS is AnkG, as demonstrated by the fact that loss of AnkG inhibits AIS assembly and maintenance of axonal characteristics in the axonal neurite (Hedstrom et al., 2007, 2008). Interestingly, we demonstrated that the location of ankG depends on the area of local TrkB activation. To provide the demonstration of how the location of AnkG is regulated, we examined the effect of BDNF on proper AIS formation in developing neurons, which we immunostained with ankG antibody (Figure 7A). Cultured DIV2 neurons, which are not yet polarized, exhibited short neurites and a few short AIS segments, whereas DIV6 neurons exhibited longer neurites and AIS structures, and thus had a higher polarity index of AnkG. Interestingly, blocking BDNF with a BDNF antibody significantly decreased AnkG staining and the polarity index (Figure 7B). These results suggest that BDNF-TrkB signaling is involved in the regulation of ankG localization. Next, we examined whether local activation of OptocytTrkB regulates the localization of AnkG in DIV2-3 neurons, in which AnkG expression is not yet strongly polarized. Interestingly, local illumination with light to activate local TrkB induced an increase in AnkG levels and translocation of AnkG from its

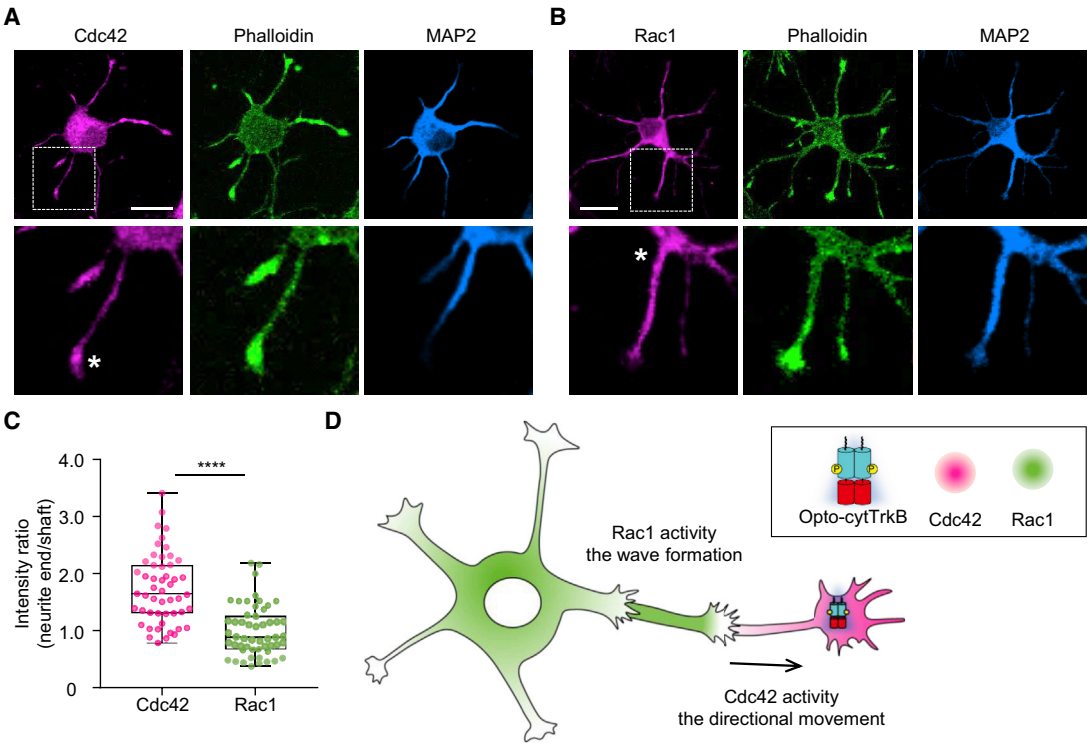

Figure 6. Regulation of Actin Waves by Preferentially Localized Cdc42 and Rac1 Activities

(A and B) Images of hippocampal neurons, immunostained with Cdc42 or Rac1 (magenta), F-actin marker phalloidin (green), and neuron marker MAP2 (light blue). Cdc42 (A) is mainly found at neurite ends (asterisk), whereas Rac1 (B) is localized mostly in the somatodendritic region (asterisk). Scale bars, 20 μm.

(C) Summary data showing localization of endogenous Cdc42 and Rac1. Data are expressed as the ratio of fluorescence intensity at the F-actin-enriched growth cone to the intensity at the neurite shaft. Data are presented as means ± SEM (Cdc42, n = 51; Rac1, n = 53; ****$p < 0.0001$; two-tailed t test).

(D) Illustration depicting Cdc42 and Rac1 activities with local TrkB activation.

See also Figure S6.

initial location to the illuminated area (Figures 7C, S7A, and S7B). Collectively, these data suggest that local BDNF-TrkB activation regulates AnkG to promote development of AIS structures in developing neurons.

Recruitment of Axonal Proteins to Form Major Neurites

We then examined whether other axonal molecules are recruited to local TrkB-activated neurites, similar to AnkG recruitment, to transform these neurites into potent axons. If local TrkB activation can cause relocation of such proteins, it is safe to assume that local TrkB activity could help determine axonal neurites or influence the fate of neurites such that they are redirected from a minor neurite fate (potential to-be dendrites) to major neurites (potential to-be axons). For neurites to develop into axons, other axonal proteins must be transported into them. Here we investigated the following axonal proteins: (1) EB3 (microtubule plus-end binding protein 3); (2) Tau, a microtubule-associated protein; (3) DrebrinE (developmentally regulated protein E), an actin-binding protein; and (4) synaptophysin, a presynaptic vesicle marker. EB3 is one of the microtubule plus-end binding proteins, and axonal microtubules are known to arranged in a uniform plus-end orientation (Stone et al., 2008). Upon local light illumination, EB3 was efficiently relocated to the local TrkB-activated neurite (Figure 7D). Tau was also translocated to the TrkB-stimulated neurite, as decreasing Tau's signal in the opposite neurites and DrebrinE was translocated likewise (Figures 7E and S7C). To verify the relationship between axonal determination and local TrkB activity more, we examined a presynaptic protein, synaptophysin, together with F-actin waves (Figure S7E). Local TrkB activation induced the formation of waves that were rich in F-actin while simultaneously filling the neurite with synaptophysin. Overall, locally activated Opto-cytTrkB resulted in a remarkable increase in the level of various axonal proteins at stimulated neurites and caused a corresponding reduction at unstimulated neurites (Figures 7F, S7D, and S7F). Therefore, our data point to a significant link between local TrkB activation and initiation of a neurite's axonal fate through acquisition of axonal properties.

DISCUSSION

In this study, we found that local TrkB activity regulates the original fate of a neurite in developing neurons by enabling it to acquire axonal properties. We leveraged the advantages of an optogenetic approach by applying a light-inducible TrkB receptor module, termed Opto-cytTrkB (Chang et al., 2014). We were able to control TrkB activity in a spatiotemporal manner, restricting TrkB activation to a light-illuminated local area. Interestingly, a stimulus limited to the distal area of neurites affected the emergence of actin waves at the proximal area. We showed that local

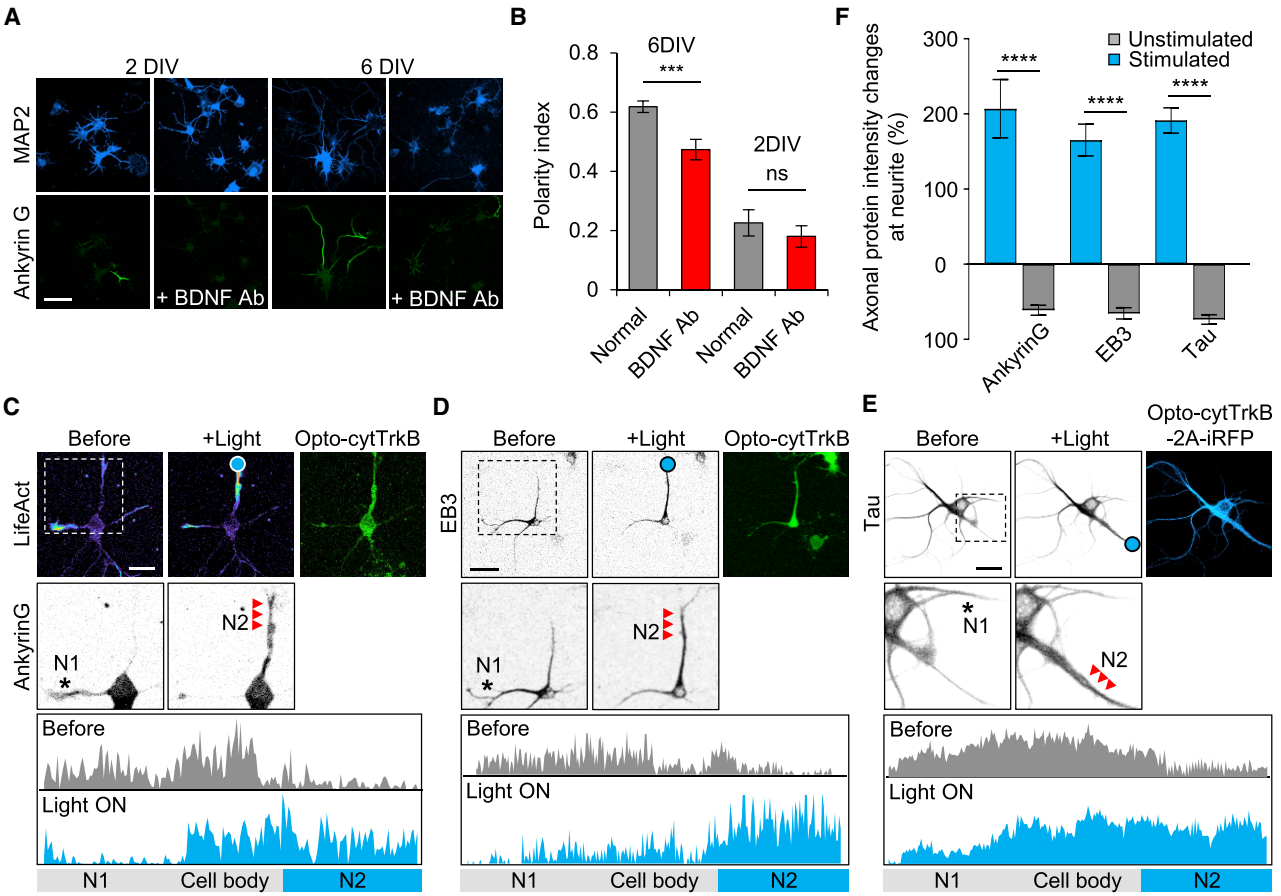

Figure 7. Rearrangement of Axonal Proteins in Local Light-Activated Neurites

(A) Images of MAP2 and AnkG immunostaining, with or without BDNF sequestration using an anti-BDNF antibody (5 μg/mL), in DIV2- and DIV6-cultured hippocampal neurons. Scale bar, 50 μm.

(B) Neuronal polarity index. Data are presented as means ± SEM (n > 35; ***p = 0.0005; ns, not significant; two-tailed t test).

(C) Re-localization of AnkG after local Opto-cytTrkB activation in young hippocampal neurons. A cultured hippocampal neuron expressing Opto-cytTrkB, iRFP682-LifeAct, and AnkG-mScarlet was locally light-illuminated (blue circle). AnkG localization in neurite 1 (N1; before illumination) and in neurite 2 (N2; after illumination) is indicated by a black asterisk and red arrowheads, respectively. Bottom panels: AnkG intensity profile before and after light stimulation. Scale bar, 20 μm.

(D) Re-localization of EB3 after local TrkB activation (blue circle). EB3 localization in neurite 1 (N1; before illumination) and neurite 2 (N2; after illumination) is indicated by a black asterisk and red arrowheads, respectively. Bottom panels: EB3 intensity profile before and after light stimulation. Scale bar, 20 μm.

(E) Specific recruitment of Tau protein to the local Opto-cytTrkB-stimulated neurite (red arrowheads). The blue circle indicates light-stimulated area. Tau localization in neurite 1 (N1; before illumination) and neurite 2 (N2; after illumination) are marked by a black asterisk and red arrowheads, respectively. Bottom panels: Tau intensity profile before and after light stimulation. Scale bar, 20 μm.

(F) Quantification of changes in the intensity of axonal proteins at stimulated and unstimulated neurites in the same hippocampal neuron. Data are presented as means ± SEM (AnkG, n = 14; EB3, n = 11; Tau, n = 24; ****p = 0.0001; two-tailed t test).

See also Figure S7.

TrkB activation concentrated the amount of actin in the same stimulated neurite, in association with the creation of a growth cone and neurite extension.

We also identified molecular mechanisms underlying actin dynamics, showing that Rac1 and Cdc42 activities are key modulators of actin accumulation and actin wave movement, both of which depend on local TrkB activity. From the standpoint of local TrkB-dependent actin dynamics, we discovered that Rac1 activity is responsible for actin accumulation and actin wave formation, whereas Cdc42 activity is essential for directional wave movement in the stimulated neurite. Rac1 and Cdc42 activities in actin waves are maintained at high levels in the neurite shaft and neurite end, respectively (Winans et al., 2016). However, the endogenous localization of these GTPases and their effects on the occurrence of actin waves are not fully understood. Here, we demonstrated the preferred subcellular localization of Rac1 and Cdc42. Both endogenous Rac1 and Cdc42 were expressed around cell bodies and neurite shafts, but only Cdc42 was highly localized at neurite ends and growth cones. Our investigation of local TrkB activation using the Opto-cytTrkB system revealed that compartmentalized Rac1 and Cdc42 are responsible for the generation and directional movement of actin waves, respectively. Interestingly, local Rac1 activation using the PA-Rac1 system yielded different outcomes depending on

the activating region. High levels of Rac1 activity in the somatodendritic area effectively triggered actin waves, whereas high levels in the growth cone and intermediate area did not, reflecting the fact that actin waves are generated from the proximal neurite through local TrkB activation at the distal neurite. These observations suggest the involvement of other molecules in this process to deliver the message to Rac1 to initiate actin waves from distal neurites with high local TrkB activity. The activity of Cdc42 is high in both actin waves and growth cones (Winans et al., 2016). Here we show that Cdc42 is the key molecule that guides actin waves as they emerge from the proximal neurite. Cdc42 activity thus provides a directional sign for wave movement, as demonstrated by the fact that inhibiting Cdc42 led to a failure to organize this molecule's proper movement to the specific site where local TrkB was activated.

Previous studies investigating the relationship between neuronal polarity and actin waves have shown that stochastically arising actin waves allow neurites to explore external environments to catch polarizing factors (Arimura and Kaibuchi, 2007). In contrast, we demonstrate that the external stimulus—in this case, BDNF-TrkB signaling—initiates actin waves and thereby takes on neuronal polarity. Axon specification of a neurite prevents other neurites from becoming axons by sending negative signals back to them (Arimura and Kaibuchi, 2007; Fukata et al., 2002; Shelly et al., 2010). Instead of invoking a negative feedback signaling mechanism for blocking axonal maturation, we assume that depletion of available actin at opposite neurites causes continuous actin depolymerization. As a result, the lengths of neurites remains short while actin accumulation induces more frequent actin polymerization at a potential axonal neurite, contributing to its elongation. We also observed that local TrkB activation in the distal region influenced the recruitment of the axonal proteins such as AnkG, Tau, EB3, Drebrin E, and synaptophysin. Among these proteins, Drebrin E is an F-actin binding proteins found mostly in developing axonal growth cones that interacts with EB3, a microtubule plus-end binding protein (Geraldo et al., 2008). Because actin waves enhance microtubule-based transport, F-actin in actin waves might interact with plus-end microtubules through Drebrin E to accelerate microtubule-based transport. More importantly, polarization of neurons during maturation requires a physiological barrier that divides the area between an axon and dendrites. AnkG is the master organizer that establishes this barrier, called the AIS (Gasser et al., 2012; Hedstrom et al., 2008). However, the molecular mechanism that determines how AnkG is initially recruited to form the AIS is poorly understood. We demonstrate here that local activation of TrkB signaling in an immature neurite regulates the initial recruitment of AnkG necessary to initiate and establish polarization.

This study demonstrates that local TrkB activation adjusts a neuron's original fate from being a minor neurite into a major axonal neurite during maturation. Local TrkB activity rearranges the actin pool to promote actin accumulation and induces growth cone formation, which causes the stimulated neurite to rapidly undergo extension. These results suggest that local TrkB activity in a distal neurite affects the overall area for polarization inside developing neurons. Collectively, our study using Opto-cytTrkB in single developing neurons have revealed deep insights into the mechanisms underlying neuronal polarity.

SIGNIFICANCE

Early-stage neurons possess symmetric neurites that gradually differentiated into a functionally divided structure composed of one axon and multiple dendrites. During neuronal polarization, a single neurite dominantly acquires axonal molecules through by frequent actin waves, which determine the axonal fate of immature neurites. The BDNF-TrkB pathway, another key signaling in neuronal polarization, promotes axon differentiation by elevating local cAMP concentration and PKA activity. However, there is no direct evidence to support the identity of the upstream cue that leads to actin waves on a single neurite. In this article, we used a photoactivatable TrkB system to demonstrate that locally activated TrkB receptors at the tips of developing neurites initiate actin waves and subsequently promote neurite elongation at the activated region, thereby breaking the original symmetry. Mechanistically, we found that local optogenetic activation of Rac1 at the distal and intermediate neurite, unlike stimulation at the proximal region, was unable to generate actin waves, implying that Rac1 activity is necessary to drive actin waves in the somatic area, but not directly involved in retrograde signal activation. In contrast to these functions of Rac1, Cdc42 guided the directional movement of actin waves, as demonstrated by the random movement observed under conditions of Cdc42 inhibition. These differential contributions of Rac1 and Cdc42 to actin wave occurrence and movement were caused by the preferential localization of endogenous Rac1 and Cdc42 to different sites. These results provide functional and spatiotemporal information on BDNF-TrkB signaling-mediated actin wave generation and symmetry-breaking processes. Intriguingly, essential axonal molecules were relocated to the light-stimulated neurite during this process. Taken together, our results provide direct evidence that BDNF-TrkB signaling mediates actin wave generation and neurite extension, providing deeper insights into the mechanism underlying neuronal polarity.

STAR★METHODS

Detailed methods are provided in the online version of this paper and include the following:

- KEY RESOURCES TABLE
- LEAD CONTACT AND MATERIALS AVAILABILITY
- EXPERIMENTAL MODEL AND SUBJECT DETAILS
  - Primary Hippocampal Neuron Culture
- METHOD DETAILS
  - Reagents
  - Plasmid Construction
  - Primary Neuron Transfection
  - Immunostaining
  - Live-Imaging and Photo-Activation
- QUANTIFICATION AND STATISTICAL ANALYSIS
  - Image Processing and Analysis
  - Analysis of AnkG Polarity
- DATA AND CODE AVAILABILITY

SUPPLEMENTAL INFORMATION

Supplemental Information can be found online at https://doi.org/10.1016/j.chembiol.2019.10.006.

ACKNOWLEDGMENTS

We thank Seungkyu Son, Jinsu Lee, and Seokhwi Kim for experimental support. This work was supported by the Institute for Basic Science, Republic of Korea (no. IBS-R001-D1), the KAIST Institute for the BioCentury, Republic of Korea. This work was also supported by grants from the National Research Foundation of Korea (NRF) funded by the Ministry of Science, Republic of Korea and ICT of the Korean Government (2017R1A2A1A17069642 and 2015M3A9A7067220).

AUTHOR CONTRIBUTIONS

D.W. and W.D.H. conceived the project and W.D.H. directed the work. D.W. and Y.S. designed and performed the experiments. D.W., Y.S., H.J., S.K., and N.K. constructed the plasmids. D.W., Y.S., H.J., S.K., S.-M.P., H.L., S.L., K.-H.C., and W.D.H. discussed the data. N.K. developed the MATLAB code for quantitation. D.W., Y.S., K.-H.C., and W.D.H. wrote the manuscript.

DECLARATION OF INTERESTS

The authors declare no competing interests.

Received: April 15, 2019
Revised: August 26, 2019
Accepted: October 10, 2019
Published: October 30, 2019

REFERENCES

Arimura, N., and Kaibuchi, K. (2007). Neuronal polarity: from extracellular signals to intracellular mechanisms. Nat. Rev. Neurosci. *8*, 194–205.

Baas, P.W., and Buster, D.W. (2004). Slow axonal transport and the genesis of neuronal morphology. J. Neurobiol. *58*, 3–17.

Barnes, A.P., and Polleux, F. (2009). Establishment of axon-dendrite polarity in developing neurons. Annu. Rev. Neurosci. *32*, 347–381.

Bradke, F., and Dotti, C.G. (1999). The role of local actin instability in axon formation. Science *283*, 1931–1934.

Chang, K.Y., Woo, D., Jung, H., Lee, S., Kim, S., Won, J., Kyung, T., Park, H., Kim, N., Yang, H.W., et al. (2014). Light-inducible receptor tyrosine kinases that regulate neurotrophin signalling. Nat. Commun. *5*, 4057.

Cheng, P.L., Song, A.H., Wong, Y.H., Wang, S., Zhang, X., and Poo, M.M. (2011). Self-amplifying autocrine actions of BDNF in axon development. Proc. Natl. Acad. Sci. U S A *108*, 18430–18435.

Dent, E.W., and Gertler, F.B. (2003). Cytoskeletal dynamics and transport in growth cone motility and axon guidance. Neuron *40*, 209–227.

Difato, F., Tsushima, H., Pesce, M., Benfenati, F., Blau, A., and Chieregatti, E. (2011). The formation of actin waves during regeneration after axonal lesion is enhanced by BDNF. Sci. Rep. *1*, 183.

Dotti, C.G., Sullivan, C.A., and Banker, G.A. (1988). The establishment of polarity by hippocampal neurons in culture. J. Neurosci. *8*, 1454–1468.

Edwards, D.C., Sanders, L.C., Bokoch, G.M., and Gill, G.N. (1999). Activation of LIM-kinase by Pak1 couples Rac/Cdc42 GTPase signalling to actin cytoskeletal dynamics. Nat. Cell Biol. *1*, 253–259.

Flynn, K.C., Pak, C.W., Shaw, A.E., Bradke, F., and Bamburg, J.R. (2009). Growth cone-like waves transport actin and promote axonogenesis and neurite branching. Dev. Neurobiol. *69*, 761–779.

Freal, A., Fassier, C., Le Bras, B., Bullier, E., De Gois, S., Hazan, J., Hoogenraad, C.C., and Couraud, F. (2016). Cooperative interactions between 480 kDa ankyrin-G and EB proteins assemble the axon initial segment. J. Neurosci. *36*, 4421–4433.

Fukata, Y., Kimura, T., and Kaibuchi, K. (2002). Axon specification in hippocampal neurons. Neurosci. Res. *43*, 305–315.

Gasser, A., Ho, T.S., Cheng, X., Chang, K.J., Waxman, S.G., Rasband, M.N., and Dib-Hajj, S.D. (2012). An ankyrinG-binding motif is necessary and sufficient for targeting Nav1.6 sodium channels to axon initial segments and nodes of Ranvier. J. Neurosci. *32*, 7232–7243.

Geraldo, S., Khanzada, U.K., Parsons, M., Chilton, J.K., and Gordon-Weeks, P.R. (2008). Targeting of the F-actin-binding protein drebrin by the microtubule plus-tip protein EB3 is required for neuritogenesis. Nat. Cell Biol. *10*, 1181–1189.

Hedstrom, K.L., Xu, X., Ogawa, Y., Frischknecht, R., Seidenbecher, C.I., Shrager, P., and Rasband, M.N. (2007). Neurofascin assembles a specialized extracellular matrix at the axon initial segment. J. Cell Biol. *178*, 875–886.

Hedstrom, K.L., Ogawa, Y., and Rasband, M.N. (2008). AnkyrinG is required for maintenance of the axon initial segment and neuronal polarity. J. Cell Biol. *183*, 635–640.

Jenkins, S.M., and Bennett, V. (2001). Ankyrin-G coordinates assembly of the spectrin-based membrane skeleton, voltage-gated sodium channels, and L1 CAMs at Purkinje neuron initial segments. J. Cell Biol. *155*, 739–746.

Kim, J., Lee, S., Jung, K., Oh, W.C., Kim, N., Son, S., Jo, Y., Kwon, H.B., and Do Heo, W. (2019). Intensiometric biosensors visualize the activity of multiple small GTPases in vivo. Nat. Commun. *10*, 211.

Minichiello, L., Casagranda, F., Tatche, R.S., Stucky, C.L., Postigo, A., Lewin, G.R., Davies, A.M., and Klein, R. (1998). Point mutation in trkB causes loss of NT4-dependent neurons without major effects on diverse BDNF responses. Neuron *21*, 335–345.

Minichiello, L., Calella, A.M., Medina, D.L., Bonhoeffer, T., Klein, R., and Korte, M. (2002). Mechanism of TrkB-mediated hippocampal long-term potentiation. Neuron *36*, 121–137.

Ogawa, Y., and Rasband, M.N. (2008). The functional organization and assembly of the axon initial segment. Curr. Opin. Neurobiol. *18*, 307–313.

Rasband, M.N. (2010). The axon initial segment and the maintenance of neuronal polarity. Nat. Rev. Neurosci. *11*, 552–562.

Riedl, J., Crevenna, A.H., Kessenbrock, K., Yu, J.H., Neukirchen, D., Bista, M., Bradke, F., Jenne, D., Holak, T.A., Werb, Z., et al. (2008). Lifeact: a versatile marker to visualize F-actin. Nat. Methods *5*, 605–607.

Ruthel, G., and Banker, G. (1998). Actin-dependent anterograde movement of growth-cone-like structures along growing hippocampal axons: a novel form of axonal transport? Cell Motil. Cytoskeleton *40*, 160–173.

Ruthel, G., and Banker, G. (1999). Role of moving growth cone-like "wave" structures in the outgrowth of cultured hippocampal axons and dendrites. J. Neurobiol. *39*, 97–106.

Schelski, M., and Bradke, F. (2017). Neuronal polarization: from spatiotemporal signaling to cytoskeletal dynamics. Mol. Cell. Neurosci. *84*, 11–28.

Segal, R.A. (2003). Selectivity in neurotrophin signaling: theme and variations. Annu. Rev. Neurosci. *26*, 299–330.

Shelly, M., Lim, B.K., Cancedda, L., Heilshorn, S.C., Gao, H., and Poo, M.M. (2010). Local and long-range reciprocal regulation of cAMP and cGMP in axon/dendrite formation. Science *327*, 547–552.

Squinto, S.P., Stitt, T.N., Aldrich, T.H., Davis, S., Bianco, S.M., Radziejewski, C., Glass, D.J., Masiakowski, P., Furth, M.E., Valenzuela, D.M., et al. (1991). trkB encodes a functional receptor for brain-derived neurotrophic factor and neurotrophin-3 but not nerve growth factor. Cell *65*, 885–893.

Stiess, M., and Bradke, F. (2011). Neuronal polarization: the cytoskeleton leads the way. Dev. Neurobiol. *71*, 430–444.

Stone, M.C., Roegiers, F., and Rolls, M.M. (2008). Microtubules have opposite orientation in axons and dendrites of *Drosophila* neurons. Mol. Biol. Cell *19*, 4122–4129.

Wang, Q., and Zheng, J.Q. (1998). cAMP-mediated regulation of neurotrophin-induced collapse of nerve growth cones. J. Neurosci. *18*, 4973–4984.

Winans, A.M., Collins, S.R., and Meyer, T. (2016). Waves of actin and microtubule polymerization drive microtubule-based transport and neurite growth before single axon formation. Elife *5*, e12387.

Wu, Y.I., Frey, D., Lungu, O.I., Jaehrig, A., Schlichting, I., Kuhlman, B., and Hahn, K.M. (2009). A genetically encoded photoactivatable Rac controls the motility of living cells. Nature *461*, 104–108.

Yang, H.W., Shin, M.G., Lee, S., Kim, J.R., Park, W.S., Cho, K.H., Meyer, T., and Heo, W.D. (2012). Cooperative activation of PI3K by Ras and Rho family small GTPases. Mol. Cell *47*, 281–290.

STAR★METHODS

KEY RESOURCES TABLE

REAGENT or RESOURCE	SOURCE	IDENTIFIER
Antibodies		
Tau-1	Millipore	MAB3420; RRID:AB_94855
AnkyrinG	Santa Cruz Biotechnology	sc-12719; RRID:AB_626674
MAP2	Covance	PCK-554P-050; RRID: AB_291541
Rac1	Abcam	ab78139; RRID:AB_2175974
Cdc42	Cell Signaling	2466; RRID:AB_2078082
Alexa Fluor 488 anti-mouse	Life Technologies	A21202; RRID:AB_141607
Alexa Fluor 647 anti-chicken	Life Technologies	A21449; RRID:AB_1500594
Alexa Fluor 488 anti-rabbit	Life Technologies	A11034; RRID:AB_2576217
Alexa Fluor 594-conjugated phalloidin	Invitrogen	A12381; RRID:AB_2315633
Alexa Fluor 488-conjugated phalloidin	Invitrogen	A12379
Bacterial and Virus Strains		
DH5α competent cells	iNtRON	ITY-YE607
Chemicals, Peptides, and Recombinant Proteins		
Recombinant human BDNF	R&D Systems	248-BD
K252a	Sigma-Aldrich	K1639
LY294002	LC Laboratories	L-7962
PD0325901	Cayman Chemical	13034
IgG-Fc	R&D systems	110-HG-100
TrkB-Fc	R&D systems	688-TK-100
BDNF-Ab	Santa Cruz Biotechnology	sc-546
Rapamycin	LC Laboratories	R-5000
NSC 23766	Sigma-Aldrich	SML0952
ZCL 278	Tocris	4974
Cycloheximide	Sigma-Aldrich	C7698
Anisomycin	Alomone lab	A-520
HBSS	Gibco	14185-052
HEPES	Gibco	15630-080
Poly-L-lysine	Sigma	P2636
Neurobasal medium	Gibco	21103-049
Horse serum	Gibco	16050-122
Glutamax	Gibco	35050-061
Penicillin-streptomycin	Gibco	15140-122
B-27 supplement	Gibco	17504-044
Lipofectamine LTX	Invitrogen	15338-100
Experimental Models: Cell Lines		
Primary rat hippocampal neurons	This paper	N/A
Oligonucleotides		
2A sequence (5'- gcc acg aac ttc tct ctg tta aag caa gca gga gac gtg gaa gaa aac ccc ggt cct-3')	This paper	N/A
Drebrin-F (5'-gaa ctc gag gcc acc atg gcc ggc gtc agc-3')	This paper	N/A
Drebrin-R (5'-gaa gga tcc gga tca cca ccc tcg aag cc-3')	This paper	N/A
SYP-F (5'-tga acc gtc aga tcc gct agc gcc acc atg gac gtg gtg aat cag ctg gt-3')	This paper	N/A
SYP-R (5'-tca cca ttt ggt ggc gac cgg tca tct gat tgg aga agg agg tgg g-3')	This paper	N/A

(*Continued on next page*)

Continued

REAGENT or RESOURCE	SOURCE	IDENTIFIER
AnkG-F (5'-tga acc gtc aga tcc gct agc gcc acc atg gct cat gcc gct-3')	This paper	N/A
AnkG-R (5'-tca cca ttt ggt ggc gac cgg tgt ggg ctt tct t-3')	This paper	N/A
Recombinant DNA		
Lyn-cytTrkB-PHR-mCitrine (Optp-cytTrkB)	This paper	N/A
Optp-cytTrkB (Y515F)	This paper	N/A
Optp-cytTrkB (Y816F)	This paper	N/A
Optp-cytTrkB (K571N)	This paper	N/A
Optp-cytTrkB (D387A))	This paper	N/A
Opto-cytTrkB-2A-iRFP	This paper	N/A
DrebrinE-FusionRed	This paper	N/A
Synaptophysin-mCherry	This paper	N/A
Synaptophysin-mScarlet-i	This paper	N/A
AnkyrinG-mCherry	Dr. Christophe Leterrier	N/A
FusionRed-Tau	This paper	N/A
AnkyrinG-mScarlet-i	This paper	N/A
mCherry-Actin	This paper	N/A
CFP-FKBP-GEF (Fgd1, Tiam1, ARHGEF11)	Yang et al., 2012	N/A
BDNF-FusionRed	This paper	N/A
BDNF-pHTomato	This paper	N/A
Software and Algorithms		
Nikon imaging software	Laboratory Imaging	microscope.healthcare.nikon.com
MetaMorph software	Analytical Technologies	moleculardevices.com
Image J	NIH	imagej.nih.gov/ij/
MATLAB	MathWorks	mathworks.com/

LEAD CONTACT AND MATERIALS AVAILABILITY

Further information and requests for resources should be directed to and will be fulfilled by the Lead Contact, Won Do Heo (wondo@kaist.ac.kr).

EXPERIMENTAL MODEL AND SUBJECT DETAILS

Primary Hippocampal Neuron Culture

Pregnant Sprague Dawley (E18) female rats were sacrificed for primary neuronal cultures. The Animal Ethic Committee at the Korea Advanced Institute of Science and Technology (KAIST; Daejeon, Korea) approved all experimental procedures. In brief, we placed embryos from the rats in phosphate-buffered saline (PBS) solution to wash out surrounding blood, and then placed the embryos in Hank's Balanced Salt Solution (HBSS) (cat. no. 14185-052; Gibco)-HEPES (10 mM; cat. no 15630-080; Gibco) solution. Hippocampi were dissected from the rat embryos in HBSS-HEPES solution and incubated in 0.25% trypsin for 15 min in a 37°C water bath as tapped every 5 min. Trypsinized hippocampi were washed with 10% FBS, then 5% FBS, then 0% FBS in HBSS-HEPES solution. Hippocampi were then dissociated with a fire-polished Pasteur pipette (>15 triturations). Dissociated neurons were immediately placed in 96-well plates (Ibidi; 89626), pre-coated with 0.1mg/ml Poly-L-lysine (cat. No. P2636; Sigma) and pre-filled with a plating medium based on Neurobasal medium (cat no. 21103-049; Gibco) supplemented with 10% horse serum (16050-122; Gibco), 2% Glutamax (cat no. 35050-061; Gibco), and 1% penicillin-streptomycin (cat. no. 15140-122; Gibco). The plated hippocampal neurons were incubated at 37°C in a humidified 5% CO_2 atmosphere. The incubated plating medium was exchanged to maintaining medium, which was based on the Neurobasal medium supplemented with 2% Glutamax, 2% b-27 (cat no. 17504-044, Gibco), and 1% penicillin-streptomycin an hour after plating neurons. Information about cell line sex is unavailable.

METHOD DETAILS

Reagents

We purchased recombinant human BDNF from R&D Systems (cat. no. 248-BD). K252a (cat. no. K1639) was purchased from Sigma-Aldrich and dissolved in dimethyl sulfoxide (DMSO). LY294002, the PI3K inhibitor, was obtained from LC Laboratories

(cat. no. L-7962) and dissolved in DMSO. PD0325901, the MAPK inhibitor, was obtained from Cayman Chemical (cat. no. 13034) and dissolved in DMSO. Poly-L-lysine hydrobromide was obtained from Sigma-Aldrich (cat. no. P2636). HBSS (10×; cat. no. 14185-052) and HEPES (10 mM; cat. no. 15630-080) were purchased from Gibco. IgG-Fc (cat. no. 110-HG-100) and TrkB-Fc (cat. no. 688-TK-100) were purchased from R&D systems. BDNF-Ab (cat. no. sc-546) was obtained from Santa Cruz Biotechnology. We purchased rapamycin from LC Laboratories (cat. no. R-5000). NSC 23766 (Rac1 inhibitor) was purchased from Sigma-Aldrich (cat. no. SML0952). ZCL 278 (Cdc42 inhibitor) was obtained from Tocris (cat. no. 4974). Cycloheximide (CHX, protein synthesis inhibitor) was purchased from Sigma-Aldrich (cat. no. C7698). Anisomycin (used for blocking the formation of a peptide bond) was obtained from Alomone lab (cat. no. A-520).

Plasmid Construction

TrkB signaling mutants (Y515F and Y816F) were generated simply by replacing the cytoplasmic domain of TrkB with their mutated domains, which we generated by site-directed mutagenesis. To construct a one-vector system, we generated a 2A peptide sequence (P2A; 5'- gcc acg aac ttc tct ctg tta aag caa gca gga gac gtg gaa gaa aac ccc ggt cct-3') with oligonucleotides and inserted a iRFP682-N1 vector. Using the In-Fusion cloning system (Clontech), Opto-cyTrkB was inserted at the N-terminus of P2A-iRFP682-N1 vector for visualization. We generated the mCherry–Lifeact and iRFP670–Lifeact plasmids based on GFP–Lifeact (Riedl et al., 2008), from which the GFP sequence was replaced with mCherry sequence or iRFP682 sequence at the *Nhe*I and *BsrG*I sites. We amplified Drebrin using a PCR reaction with Drebrin-F (5'-gaa ctc gag gcc acc atg gcc ggc gtc agc-3') and Drebrin-R (5'-gaa gga tcc gga tca cca ccc tcg aag cc-3'), and inserted a FusionRed-N1 vector (Clontech) using *Xho*I and *BamH*I restriction sites. Synaptophysin-mCherry was from Syn-ATP vector (Addgene no.51819), which we cut and inserted in the EGFP-N1 vector (Clontech) using *Hind*III and *BsrG*I restriction sites. We amplified Synaptophysin through a PCR reaction with SYP-F (5'-tga acc gtc aga tcc gct agc gcc acc atg gac gtg gtg aat cag ctg gt-3') and SYP-R (5'-tca cca ttt ggt ggc gac cgg tca tct gat tgg aga agg agg tgg g-3'), inserted in a mScarlet-i-C1 vector (Addgene no.85044) using *Nhe*I and *Age*I enzyme sites. To design the mCherry-Actin construct, a human β-Actin gene was inserted with *Xho*I and *BamH*I restriction sites in the mCherry-C1 vector (Clontech). We generated BDNF-FusionRed and BDNF-pHTomato by inserting PCR amplified human BDNF (cat. no. SC108977; Origene) in FusionRed-N1 and pHTomato-N1 vectors using *EcoRI* and *BamHI* enzyme site. EB3 was inserted with *Nhe*I and *Age*I restriction sites in the mCherry-N1 vector (Clontech), which contained a flexible linker (three repeats of GGGGGGGS) at its N-terminus. Lyn-FRB and CFP-FKBP-GEFs (Fgd1, Tiam1, ARHGEF11) have been described previously (Yang et al., 2012). Dr. Christophe Leterrier (Aix Marseille Université, France) provided the AnkG-mCherry construct. To generate AnkG-mScarlet-i, PCR-amplified AnkyrinG was inserted in mScarlet-i-C1 vector with *Nhe*I and *Age*I restriction sites. The PCR reaction was performed using AnkG-F (5'-tga acc gtc aga tcc gct agc gcc acc atg gct cat gcc gct-3') and AnkG-R (5'-tca cca ttt ggt ggc gac cgg tgt ggg ctt tct t-3') primers.

Primary Neuron Transfection

We transfected cultured primary hippocampal neurons at 2-3DIV with Lipofectamine LTX and plus reagent (Invitrogen; 15338-100) in Opti-MEM (Invitrogen) following the manufacturer's instructions. In brief, 0.8 μg of DNA was incubated with 0.8 μl of plus reagent in 100 μl of Opti-MEM for 5 min, and then 0.8 μl Lipofectamine LTX reagent was added to the mixture. After incubating the mixture for 20 min at room temperature, we added 400 μl of the neuron-maintaining media (without the B-27 supplement) to the mixture. We placed 100 μl of the mixture into each well of a 96-well microplate after the incubated medium was stored separately. Next, the mixture was incubated for 40 min at 37°C in a humidified 5% CO_2 atmosphere. The incubated mixture was then entirely replaced with the pre-stored maintaining media. Time-lapse images were captured one day after transfection.

Immunostaining

Primary rat hippocampal neurons were cultured and $2x10^5$ cells were plated in each well of a 24-well plate. Three hours later, the plated neurons were incubated with BDNF (50ng/ml), K252a (100ng/ml), BDNF-Ab (5μg/ml), IgG-Fc (20 μg/ml), or TrkB-Fc (20μg/ml) for 36 hours. Then, the plated neurons were fixed with 3.5% paraformaldehyde (PFA) for 10 min at room temperature. After washing three times with 0.1% Tween-20 in phosphate buffered saline (PBS), we undertook membrane permeabilization and blocking steps at the same time using a buffer that consisted of 0.1% saponin, 1% fetal bovine serum (FBS), and 1% bovine serum albumin (BSA) in PBS for 15 min at room temperature. After another three washes with PBS, Tau-1 (1:500; MAB3420 from Millipore), AnkG (1:100, sc-12719 from Santa Cruz), and MAP2 (1:1000; PCK-5549-050 from Covance), the primary antibodies were incubated overnight in a blocking solution (1% BSA and 1% FBS in PBS) at 4°C. Both of secondary antibodies—Alexa Fluor 488 anti-mouse and 647 anti-chicken (1:2000; A21202 and A21449 respectively from Life Technologies)—were incubated together with Alexa Fluor 594-conjugated phalloidin (200×; A12381 from Invitrogen) for 90 min at room temperature in a dark condition. After washing three times with PBST (0.1% Tween-20 in PBS), we imaged the stained neurons using confocal microscopy. Immunostaining of Rac1 and cdc42 was performed in the same procedure with above-mentioned antibodies. The primary antibodies against Rac1 (1:100; ab78139 from Abcam) and Cdc42 (1:100; 2466 from Cell Signaling) were used and then visualized with Alexa Fluor 488 anti-rabbit (1:2000; A11034 from Life Technologies) and Alexa Fluor 488-conjugated phalloidin (100×; A12379 from Invitrogen).

Live-Imaging and Photo-Activation

We imaged the transfected neurons a day after transfection. We performed live-cell imaging using a Nikon A1R confocal microscope (Nikon Instruments) mounted onto a Nikon Eclipse Ti body that is equipped with CFI Plan Apochromat VC objectives (60×/1.4-NA oil

or 40×/0.95-NA air; Nikon) and a Chamlide TC system (maintained at 37°C and 10% or 5% CO_2; Live Cell Instrument, Inc.). mCitrine, mCherry, iRFP, and GFP images were captured with 514, 561, 640, and 488-nm lasers, respectively. We used a Nikon built-in photo-activation set for light illumination and a 488-nm laser for photo-stimulation. The laser light intensity was measured right above the objective by an optical power meter (cat. no. 8230E; ADCMT, Japan). The measured optical power ranged from 5 to 20 μW (110-440 μW mm^{-2}) for photo-activation. To illuminate the whole area (512×512 μm with 60× lens/no zoom and 2 seconds of time), we used 20 μW (detected by ADCMT above the objective) of 488 nm light power (440 μW mm^{-2}). To stimulate a local area (4×4 μm with 60 × lens/no zoom and 300 milliseconds of time), we used 5 μW (110 μW mm^{-2}) of 488 nm light power. The images were analyzed with Nikon imaging software (NIS-element AR 64-bit version 3.10; Laboratory Imaging) and Image J (Fiji) software.

QUANTIFICATION AND STATISTICAL ANALYSIS

Image Processing and Analysis

All images were analyzed with Nikon imaging software (NIS-element AR 64-bit version 4.10; Laboratory Imaging) and MetaMorph software (version 7.7; MDS Analytical Technologies). To draw the kymographs and intensity plot, we used the 'Create Kymograph by Line' and 'Intensity profile' tools, respectively, in NIS software. Inverted images were modified in Image J, using the 'Invert LUT' tool. We measured the growth cone area with the 'Auto detect ROI' tool in NIS software. Actin intensity profiles were analyzed with the 'Plot profile' function in Image J software. The intensity changes of F-actin and proteins at the region of interest was measure by 'Time measurement' tools. Statistical significance was evaluated using a two-tailed Student's t-test using the GraphPad Prism. The one-way anova with Tukey multiple comparisons test was used to determine the pvalues between three or more groups of data.

Analysis of AnkG Polarity

We developed a customized MATLAB code for analyzing image data as described previously (Freal et al., 2016). We calculated polarity index by using immunostained fluorescence intensities of AnkG and MAP2. The intensities of axons and dendrites were defined by fluorescence signals of AnkG and MAP2, respectively, in the 20 μm of the neurites from the soma.

DATA AND CODE AVAILABILITY

The published article includes all datasets generated or analyzed during this study.